LBL-21383
Preprint c.2

Lawrence Berkeley Laboratory
UNIVERSITY OF CALIFORNIA

RECEIVED
LAWRENCE
BERKELEY LABORATORY

SEP 16 1986

LIBRARY AND
DOCUMENTS SECTION

Submitted to Nuclear Physics

ESTIMATES OF THE INFLUENCE OF NUCLEAR DEFORMATIONS AND SHELL EFFECTS ON THE LIFETIMES OF EXOTIC RADIOACTIVITIES

Y.-J. Shi and W.J. Swiatecki

March 1986

TWO-WEEK LOAN COPY
This is a Library Circulating Copy which may be borrowed for two weeks.

NUCLEAR SCIENCE DIVISION

LBL-21383 c.2

Prepared for the U.S. Department of Energy under Contract DE-AC03-76SF00098

DISCLAIMER

This document was prepared as an account of work sponsored by the United States Government. While this document is believed to contain correct information, neither the United States Government nor any agency thereof, nor the Regents of the University of California, nor any of their employees, makes any warranty, express or implied, or assumes any legal responsibility for the accuracy, completeness, or usefulness of any information, apparatus, product, or process disclosed, or represents that its use would not infringe privately owned rights. Reference herein to any specific commercial product, process, or service by its trade name, trademark, manufacturer, or otherwise, does not necessarily constitute or imply its endorsement, recommendation, or favoring by the United States Government or any agency thereof, or the Regents of the University of California. The views and opinions of authors expressed herein do not necessarily state or reflect those of the United States Government or any agency thereof or the Regents of the University of California.

LBL-21383

Estimates of the influence of nuclear deformations and shell effects on the lifetimes of exotic radioactivities

Y.-J. Shi* and W.J. Swiatecki

Nuclear Science Division
Lawrence Berkeley Laboratory
University of California
Berkeley, California 94720

March, 1986

This work was supported by the Director, Office of Energy Research, Division of Nuclear Physics of the Office of High Energy and Nuclear Physics of the U.S. Department of Energy under Contract No. DE-AC03-76SF00098.

*Permanent address: Institute of Atomic Energy, P.O. Box 275 (18), Beijing, China.

LBL-21383

Estimates of the influence of nuclear deformations and shell effects on the lifetimes of exotic radioactivities

Y.-J. Shi* and W.J. Swiatecki

Nuclear Science Division
Lawrence Berkeley Laboratory
University of California
Berkeley, California 94720

March, 1986

Abstract

We estimate the influence on the lifetimes of exotic radioactivities of nuclear ground-state deformations and of the attenuation of fragment shell effects by the fragments' interaction. These corrections are generally of the order of one power of ten, representing modifications of the barrier penetrabilities amounting to a few percent. The corrections to the lifetimes do not ruin the current reasonable correspondence between theory and experiment. In fact, the fit is improved slightly.

This work was supported by the Director, Office of Energy Research, Division of Nuclear Physics of the Office of High Energy and Nuclear Physics of the U.S. Department of Energy under Contract No. DE-AC03-76SF00098.

*Permanent address: Institute of Atomic Energy, P.O. Box 275 (18), Beijing, China.

1. Introduction

Exotic radioactivity (the very asymmetric spontaneous decay of nuclei by the emission of fragments heavier than α particles) was anticipated on theoretical grounds and was subsequently confirmed by experiment. For a review of the history of this topic and for tabulations of the data, see refs. 1-3. At this time there exist eight reported cases of such radioactivity and seven significant lower limits on the lifetimes (see Table I and Figs. 1,2). On the theoretical side, there are available the extensive surveys described in[1,2] as well as the estimates of the present authors in[4,5]. In the latter work an attempt was made to estimate the decay lifetimes and their ratios to α-decay in a way free of any adjustable parameters. The calculations were based on Gamow penetrability factors for one-dimensional barriers constructed as follows. Beyond the contact or scission configuration, the barrier was obtained by adding the nuclear proximity attraction to the electrostatic repulsion between the decay products (assumed spherical). In the relatively narrow range between the contact configuration and the parent configuration (which was also assumed to be spherical and whose mass is known experimentally), the barrier (or, equivalently, the integrand in the Gamow penetrability formula) was obtained by a smooth power-law interpolation. The resulting ratios of the calculated penetrability factors for exotic decay and for α-decay are compared with the measured branching ratios for these two modes in Fig. 1. Fig. 2 shows the calculated exotic penetrabilities themselves, together with empirical values deduced by dividing the observed exotic half-lives by a pre-exponential factor (taken to be 10^{-22}sec for even-A and 10^{-20}sec for odd-A parent nuclei). The degree of correspondence of theory and experiment is within about two orders of magnitude in Fig. 1 and one order of magnitude in Fig. 2, which would imply that the penetrability integrals have been estimated correctly to within a few percent. (An error of one power of ten in the lifetime for ^{14}C emission from Ra translates into an error of about 3% in the penetrability integral.) In order to learn whether this degree of agreement represents the essential correctness of the underlying physical assumptions or, on the contrary, whether it is the result of accidental cancellations of large corrections, it is of interest to estimate the effect on the

theoretical predictions of known or anticipated deviations from the idealized model used in refs. 4,5.

The present paper deals with two such refinements: 1) the known deviations from sphericity of the parent and/or daughter nuclei and 2) the anticipated attenuation of the fragment ground-state shell effects caused by the nuclear interaction between the fragments. In the course of this analysis we have also confirmed the existence of systematic odd-even effects in the exotic half-lives, as already noted in ref. 3.

2. The Effect of Deformations

We shall restrict our attention to the case of most practical relevance, in which the emitted fragment is still considered spherical, but the parent and/or daughter may have an axially symmetric deformation. The potential-energy barrier will now depend on the polar angle θ between the axis of symmetry of the daughter or parent nucleus and the direction of the emitted fragment (see Fig. 3).

In analogy with refs. 4,5 we construct the post-contact (post-scission) barrier at each angle θ by adding to the electric repulsion the proximity attraction between the fragments. (Both interactions are now affected by the daughter's deformation.) This estimate of the barrier is used down to contact or, more precisely, down to the point where the separation between the centers of the fragments is equal to the sum of the radius of the emitted fragment and the radius vector of the daughter's surface at the angle θ. (In the case of a deformed daughter, this point is just a shade inside the true contact configuration, as may be seen from Fig. 3. Having noted this here we shall, nevertheless, go on referring to this point as the contact or scission configuration for the angle θ.) Again in analogy with refs. 4,5 we shall construct the pre-scission part of the barrier at the angle θ by smooth interpolation between the contact configuration and the parent configuration.

Denote the radius vectors specifying the surfaces of the parent and daughter by $C(\theta)$ and $C_1(\theta)$ respectively, and the radius of the emitted fragment by C_2. As in refs. 4,5 take as the disintegration variable at each angle θ the total extension L of the system, as measured along the

radius vector specified by θ. The contact configuration corresponds to

$$L_c = 2(C_1(\theta)+C_2) \tag{1}$$

and the initial parent configuration corresponds to L_o where

$$L_o = 2C(\theta) \quad . \tag{2}$$

For an arbitrary post-scission configuration specified by L, the separation θ between the centers of the fragments is given by

$$r = L - C_1(\theta) - C_2 \tag{3}$$

and the separation s between their surfaces (along the direction θ) is

$$s = L - 2(C_1(\theta)+C_2) \quad . \tag{4}$$

For $L = L_c$ the potential-energy barrier appropriate to disintegration in the θ-direction is now written as

$$V(L,\theta) = M_1+M_2-M+V_C(r,\theta)+V_P(s,\theta) \tag{5}$$

where M_1,M_2 and M are the masses of the fragments and the parent nucleus, respectively, and V_C and V_P are the Coulomb and proximity energies, given explicitly in the appendix.

For $L_o < L < L_c$ the same power law interpolation for $V(L,\theta)$ is assumed as in refs. 4,5:

$$V(L,\theta) = a(L-L_o)^\nu \quad , \tag{6}$$

where the parameters a,ν are determined (at each angle) by the requirement of a smooth fit at $L = L_c$.

Without referring to the explicit formulae in the appendix, the qualitative effects of parent and daughter deformations on the penetrabilities of interest may be described as follows. If the parent is deformed but the daughter is spherical (approximately the case of ^{14}C emission from Ra and of other exotic radioactivities) the post-scission part of the barrier is unaffected but the pre-scission part for polar emission is thinner compared to equatorial emission (in the case of a prolate deformation of the parent). If both the parent and daughter have the same deformation (approxi-

mately the case for α-emission from well-deformed nuclei) the post-scission barrier is lower and thinner for polar emission compared to equatorial emission, while the width of the pre-scission barrier is approximately independent of angle.

An estimate of the decay lifetime can be obtained by a suitable average over all directions of emission. Thus, in the simplest treatment of radioactive decay, the attenuation of the wave-function amplitude referring to decay along the θ direction will be dominated by the barrier penetration factor

$$\exp\left[-\frac{1}{\hbar}\int_{L_o}^{L_e}\sqrt{2M_r V}\;dL\right] \quad , \tag{7}$$

where L_e is the exit point defined by $V(L_e,\theta)=0$ and M_r is the effective inertial mass associated with the disintegration degree of freedom (equal, in the post-scission regime, to the reduced mass of the separating fragments). The square of the angle-averaged attenuation factor governs the decay probability, and an estimate for the decay lifetime τ follows as

$$\tau = \tau_o\, G \quad , \tag{8}$$

where

$$G^{-1} = \left\{\int_0^1 d\,(\cos\theta)\exp\left[-\frac{1}{\hbar}\int_{L_o}^{L_e}\sqrt{2M_r V}\;dL\right]\right\}^2 \tag{9}$$

and τ_0^{-1} is a barrier assault frequency for the process in question. In order of magnitude, τ_o is expected to be given by the period of collective nuclear (quadrupole) oscillations in the case of conventional fission ($\sim 10^{-21}$sec). It is expected to decrease somewhat with increasing asymmetry of the division, on account of the decreasing characteristic wavelength and period of the deformation describing the incipient formation of a smaller fragment.

It is important to stress that we do not imply that the effective inertia M_{eff} in the pre-scission regime is equal to the reduced mass M_r. Since it is only the *product* $M_{eff}\ V$ that enters the penetrability formula, our procedure is fully equivalent to a smooth interpolation of $M_{eff}\ V$ according to the power law described by eq. (6). Thus, in place of eq. (6), we can equally well write

$$M_r\ V(L\ ,\theta) = aM_r\,(L - L_0)^{\nu} = a'\ (L - L_0)^{\nu}\ ,$$

where a' and ν are determined by the requirement of a smooth fit at $L = L_c$. All numerical results remain strictly unaltered by this change in point of view, according to which $M_{eff}\ V$ is taken to be $M_r\ V$ in the post-scission regime, but no statement is made about the separate values of M_{eff} and V in the pre-scission regime.

3. The Attenuation of Fragment Shell Effects

The energy release (or Q-value) in a disintegration is given by eq. (5) as

$$Q = M - M_1 - M_2 \quad . \tag{10}$$

Because the nuclear masses M, M_1, M_2 contain shell effects, the resulting barriers and penetrabilities reflect these effects directly. (It is precisely because of the strong shell effect in the daughters, dominated by the magic numbers $Z = 82$ and $N = 126$ that, in agreement with theoretical expectations, all the exotic decays seen so far lead to residual nuclei in that vicinity.) It is clear, however, that the use of eq. (5), where the fragment shell effects do not depend on the separation of the two nuclei, is likely to underestimate somewhat the barrier and to overestimate the shell-effect enhancement of a decay into magic nuclei. The reason is that, as two nuclei begin to interact and their surfaces interpenetrate around contact, their shell effects are bound to be attenuated. Later, as the nuclei amalgamate, these shell effects will even be destroyed entirely, to be replaced eventually by the shell effect of the fused parent nucleus. In order to estimate the attenuation of the shell effects caused by the fragment interaction, we have developed the following scheme, analogous in spirit to the semi-quantitative treatment of the attenuation of shell effects by nuclear deformations, which underlies the description of nuclear masses and deformations in refs. 6,7.

Disregarding at first the diffuseness of the nuclear density distributions, imagine two sharp-surfaced nuclei with radii C_1 and C_2, each with its characteristic surface energy $E_{S1} = 4\pi C_1^2 \gamma$ and $E_{S2} = 4\pi C_2^2 \gamma$, and extra shell-effect contributions to the binding, which we shall denote by $S_1(\infty)$ and $S_2(\infty)$. (The quantity γ is the specific surface energy.)

If, slightly after contact, the shape of the nucleus (and of the sharp dinuclear potential well) is taken to be that of portions of two slightly overlapping spheres, communicating through a window of radius c, the total surface energy will be reduced by $2\pi c^2\gamma$. As regards the shell effects S_1 and S_2, they may be expected to suffer an attenuation proportional to the area πc^2, which is a measure of the degree of communication between the two nuclear potential wells. Moreover, since S_1 may be expected to be destroyed completely when πc^2 is of the order πC_1^2, and S_2 when πc^2

is of the order πC_2^2 , one may try as an estimate of the shell effects at the stage when the window radius is c the following expression:

$$S_i \approx S_i(\infty)\left(1-\frac{c^2}{C_i^2}\right) = S_1(\infty)\left(1+\frac{V_{int}}{2\pi C_i^2\gamma}\right) \quad \text{for} \quad c = C_i \quad , \tag{11}$$

where V_{int} is the interaction energy (the decrease below the energy of non-interacting spheres) given by

$$V_{int} = -2\pi c^2\gamma \quad . \tag{12}$$

By elementary geometry, the window radius c is related to the (small) degree of overlap of the spheres (denoted by $-s$) by

$$c^2 = 2\overline{R}(-s) \quad , \tag{13}$$

where $\overline{R} = C_1C_2/(C_1+C_2)$, so that the interaction energy may also be written as

$$V_{int} = \begin{cases} 4\pi\overline{R}\,\gamma s & \text{for } s < 0 \\ 0 & \text{for } s \geq 0 \end{cases} \quad . \tag{14}$$

A straightforward generalization of the shell-attenuation factor in eq. (11) to the case of diffuse surfaces immediately suggests itself: replace V_{int} in that equation by the proximity interaction V_P , whose role is precisely to generalize the interaction given by eq. (14) to the case of diffuse surfaces. According to refs. 8,9,10 we have

$$V_P(s) = 4\pi\overline{R}\,\gamma b\,\Phi(\varsigma) \quad , \tag{15}$$

where $\varsigma = s/b$, b is the Sussmann width (diffuseness) of the surface and Φ is the universal dimensionless nuclear proximity function, to which a conventional approximation is given in the appendix. It is readily verified that as the diffuseness b tends to zero, V_P tends essentially to V_{int} given by eq. (14) and thus vanishes for $s > 0$. But, in general, V_P is finite for $s > 0$ and it is in fact in this post-scission regime that we shall use eq. (15) to estimate the effect of shell attenuation on the exotic radioactivity. The logic here is that V_P continues to provide in the post-scission regime a measure of the degree of communication between the two diffuse nuclei, which communication tends to destroy the individual shell effects characteristic of non-interacting

systems.

Using the above formulae, one readily verifies the following two ways of writing the expression that generalizes eq. (5) for the shell-attenuation effect:

$$V(L,\theta) = M_1 + M_2 - M + V_C + \mu V_P \quad , \tag{16}$$

where

$$\mu = 1 + \frac{2S_1(\infty)}{E_{S1}} + \frac{2S_2(\infty)}{E_{S2}} \quad , \tag{17}$$

or

$$V(L,\theta) = D_1 + D_2 - M + V_C + V_P$$
$$+ S_1(\infty)\left(1 + \frac{2\bar{R}b}{C_1^2}\,\Phi(\varsigma)\right) + S_2(\infty)\left(1 + \frac{2\bar{R}b}{C_2^2}\,\Phi(\varsigma)\right) \quad , \tag{18}$$

where D_1 and D_2 are the macroscopic (e.g. Droplet Model) parts of the fragment masses, so that $M_1 = D_1 + S_1(\infty)$ and $M_2 = D_2 + S_2(\infty)$.

Eq. (18) shows explicitly how the original shell effects are attenuated as the two nuclei approach. Eq. (16) shows that, operationally, our prescription for the shell attenuation results merely in a (slight) modification of the strength of the proximity interaction!

In order to illustrate the magnitude of the shell-attenuation effect in a typical case, take the exotic decay of ^{222}Ra into ^{208}Pb and ^{14}C. According to ref. 7 the shell effect in ^{208}Pb is $S_1(\infty) = -13.42$ MeV and, using the canonical parameter set explained in the appendix, the corresponding attenuation factor at contact is

$$1 + \frac{2\bar{R}b}{C_1^2}\,\Phi(0) = 1 - 0.131 \quad . \tag{19}$$

Thus the ^{208}Pb shell effect is reduced by a modest 13% or about 1.76 MeV. The shell effect of a light nucleus like ^{14}C is not easily estimated (on account of the difficulty of defining a smooth macroscopic energy, whose subtraction from the experimental mass would give the shell effect). Taking at face value the method of estimating shell effects for light nuclei described in sec. 7.3 of

ref. 6, the nominal shell effect for ^{14}C turns out to be $S_2(\infty) = -0.56$ MeV. The attenuation factor comes out to be close to zero at contact, so this small extra binding would be destroyed there. For even lighter nuclei, such as the α-particle, the definition of a shell effect is quite ambiguous and the use of the proximity formalism is only marginally justified (see ref. 8). For the sake of uniformity, when estimating decay branching ratios, we shall nevertheless apply the shell-attenuation formula also to the α-particle, but with the modification that we shall not allow the attenuation factor to become negative. (This would imply, without any physical justification, a reversal in the *sign* of the shell effect.) In cases where the nominal attenuation function $1 + \frac{2\overline{R}b\,\Phi(\varsigma)}{C_i^{\,2}}$ does turn negative before contact (as it does for the α-particle) we shall adopt the convention of replacing it by $\left(1 - \frac{\Phi(\varsigma)}{\Phi(0)}\right)$, which forces the disappearance to occur *at* contact. Thus our attenuation of a shell effect in nucleus i will be described by

$$S_i = \begin{cases} S_i(\infty)\left(1 + \frac{2\overline{R}b}{C_i^{\,2}}\,\Phi(\varsigma)\right) & \text{if } 1 + \frac{2\overline{R}b}{C_i^{\,2}}\,\Phi(0) > 0 \\ S_i(\infty)\left(1 - \frac{\Phi(\varsigma)}{\Phi(0)}\right) & \text{if } 1 + \frac{2\overline{R}b}{C_i^{\,2}}\,\Phi(0) < 0 \end{cases} \quad . \tag{20}$$

(The second line is relevant only for nuclei lighter than about carbon.)

According to ref. 6 the nominal shell effect for the α-particle is -1.51 MeV and, according to eq. (20), this would be destroyed at contact with a heavy nucleus. On the other hand, eq. (20) would suggest that the shell effect of ^{218}Rn (-3.58 MeV according to ref. 7) would be reduced by a mere 0.27 MeV through contact with an α-particle.

It will be clear that our prescription for the shell-attenuation effect is only the roughest kind of starting point, with large quantitative uncertainties. To gain more flexibility in writing down the shell attenuation form factor $[1+(V_P/2\pi\overline{R}^2\gamma)]$ we might well have allowed ourselves one or two adjustable parameters to govern the strength and/or range of the attenuation function (see also appendix). We prefer, however, to avoid at this stage the introduction of any undetermined factors and to retain the parameterless baseline estimate given by eq. (20). As our understanding

of the shell attenuation effect improves with time, the need for improving this baseline estimate will surely emerge.

4. Results

If the simple lifetime formula, eq. (8), were exact, a plot of the experimental τ divided by the calculated G would be a constant, independent of the disintegrating system. Figures 4 and 5 show the degree of correspondence with this expectation when our calculated values of G_α and G_X are used. The top part of Fig. 4 shows log (τ_α/G_α), i.e., log τ_0^α, with τ_0^α in sec. The dashed lines refer to the "old" calculations without corrections for deformation and shell-attenuation effects. The solid lines ("new" calculation) include such corrections. In both cases the values of τ_0^α are spread over two orders of magnitude, but it is immediately clear that much of this spread is due to an odd-even effect, the odd-A nuclei in question having τ_0^α values longer on the average than even-A nuclei. The lower part of Fig. 4 displays the corresponding plots of log τ_0^X for the exotic radioactivities. An even larger odd-even effect is apparent. The averages and RMS deviations from a constant of the eight plots in Fig. 4 are as follows:

For α-radioactivity

$$<\log \tau_0^\alpha>_{odd}^{old} = -21.45 \pm 0.51 \rightarrow \tau_0^\alpha = 3.55\times10^{-22}\text{sec}$$

$$<\log \tau_0^\alpha>_{odd}^{new} = -21.73 \pm 0.45 \rightarrow \tau_0^\alpha = 1.86\times10^{-22}\text{sec}$$

$$<\log \tau_0^\alpha>_{even}^{old} = -22.42 \pm 0.29 \rightarrow \tau_0^\alpha = 3.80\times10^{-23}\text{sec}$$

$$<\log \tau_0^\alpha>_{even}^{new} = -22.66 \pm 0.17 \rightarrow \tau_0^\alpha = 2.19\times10^{-23}\text{sec}$$

$$<\log \tau_0^\alpha>_{odd} / <\log \tau_0^\alpha>_{even} = \begin{Bmatrix} 0.97 & old \\ 0.93 & new \end{Bmatrix} \approx 1 \quad .$$

For exotic radioactivity

$$<\log \tau_0^X>_{odd}^{old} = -20.09 \pm 0.48 \rightarrow \tau_0^X = 8.13\times10^{-21}\text{sec}$$

$$<\log \tau_0^X>_{odd}^{new} = -20.36 \pm 0.40 \rightarrow \tau_0^X = 4.37\times10^{-21}\text{sec}$$

$$<\log \tau_0^X>_{even}^{old} = -21.88 \pm 0.63 \rightarrow \tau_0^X = 1.32\times10^{-22}\text{sec}$$

$$<\log \tau_0^X>_{even}^{new} = -22.32 \pm 0.71 \rightarrow \tau_0^X = 4.79\times10^{-23}\text{sec}$$

$$<\log \tau_0^x>_{odd} / <\log \tau_0^x>_{even} = \begin{Bmatrix} 1.79 & old \\ 1.96 & new \end{Bmatrix} \approx 2 \quad .$$

In round figures then, the pre-exponential factor for exotic decays of even-A nuclei is $\tau_0^X \approx 10^{-22}$sec when the old calculation is used for G_X and 0.5×10^{-22}sec for the new calculation; the odd-A exotic decays are hindered by about two powers of 10.

Figure 5 shows separately the effect on log τ_0^X of including in the calculation the shell attenuation (upper part) and deformations (lower part). The former lowers τ_0^X by about an order of magnitude. The latter has little effect for the lighter nuclei but increases τ_0^X by about an order of magnitude for the most strongly deformed, heaviest isotopes.

Figure 6 shows a comparison of the experimentally deduced values of G_X with the "new" calculations (compare Fig. 1). With the odd-even effect included and allowances made for shell attenuation and for deformations, there are now almost no significant deviations between theory and experiment. The largest deviation is in the case of ^{232}U $\rightarrow$ ^{208}Pb + ^{24}Ne, where the observed branching ratio to α-decay, given as $(2.0 \pm 0.5) \times 10^{-12}$, leads to a value of log G_X greater by 1.32 than our estimate. This is a factor 20 discrepancy in the lifetime, equivalent to a 3% error in the estimated penetrability. In the remaining 7 measured cases the discrepancy is usually well under a factor of 10. The RMS deviation for all 8 cases is 0.62, corresponding to a factor 4 average discrepancy. This is just about the same as the average discrepancy associated with the old calculation (Fig. 1). The slight improvement of the new over the old fit consists in the absence of discrepancies with lower limits on the lifetimes. (In Fig. 1 there are two -- barely significant -- discrepancies, for ^{221}Fr and ^{221}Ra.) Also, the old calculation predicts that the most favoured exotic decay of ^{230}Th should be by the emission of ^{22}O, with emission of ^{24}Ne a factor of 9.8 less

frequent. By contrast, the new calculation predicts ^{24}Ne to be the most favoured case, in agreement with observation. The emission of ^{22}O is now a factor of 5.5 *less* frequent. Thus, with the new calculation, the anticipated most favoured decay is, without exception, the one actually observed.

Whether these relatively slight improvements are really significant is not clear -- the principal message is that the introduction of the refinements considered here does not *ruin* the correspondence between theory and experiment.

5. Discussion

The present study suggests that our simple one-dimensional treatment of exotic radioactivity does not owe its relative accuracy to accidental cancellations of large errors: the results appear quite stable with respect to inclusion of shell-attenuation and deformation effects. Even though our estimate of these corrections (as corresponding to about a factor of ten) must be regarded as very rough, we feel it is unlikely that these corrections could possibly change the original lifetime estimates by *several* powers of 10. The fact that even the largest ground-state deformations in the heavy actinide region enhance the lifetimes by no more than about a factor of 10 shows that the occurrence of exotic radioactivity is not to be thought of as associated specifically with such deformations. In particular, the occurrence of octupole deformations in the Ra region should not be regarded as the explanation of the exotic disintegrations with the emission of a C fragment. Such disintegrations are expected to occur with about the same frequency (on a logarithmic scale) whether the parent nucleus is deformed or not. The simple reason for this relative insensitivity to deformations is that, in the case of these very asymmetric disintegrations, most of the barrier corresponds to separating fragments, and the parent deformation affects only the relatively small pre-scission part. Note, however, that this situation is expected to change as one goes to more symmetric divisions. Thus, in the case of normal spontaneous fission of deformed nuclei, the barrier to be penetrated is very much narrower than it would be in the absence of ground state deformations.

In this connection we should also stress that we have only considered the effects of *ground-state* deformations. Deformations (around scission) induced by the mutual interactions between the fragments (and, more generally, by the dynamics of the disintegration process) have not been discussed at all. Again, in the case of normal fission, such deformations have an overwhelming effect on the spontaneous fission lifetimes. This makes it quite certain that our one-dimensional treatment of exotic radioactivity, based on spherical fragments beyond scission, is bound to fail as more symmetric divisions are considered. This failure would be mitigated in the case of magic fragments with their propensity for spherical shapes but, in general, one is faced, as in fission, with the discussion of barrier penetrabilities in two or more dimensions. This is a problem vastly more difficult than our one-dimensional treatment, which owes its relative accuracy to the extreme asymmetry of the division and, surely, also to the stiffness of the spherical daughter in the vicinity of the doubly magic ^{208}Pb nucleus. In the absence of more comprehensive multi-dimensional penetrability estimates, one should at least be aware of the serious limitations of the one-dimensional treatment and one should be prepared for large discrepancies in the case of more symmetric disintegrations, especially those involving non-magic fragments.

Acknowledgements

We are particularly indebted to P.B. Price and S.W. Barwick for keeping us abreast of the experimental situation and for many valuable suggestions. We would like to thank J.O. Rasmussen for enlightening discussions concerning α-decay of deformed nuclei. One of us (Y-J.S.) would like to acknowledge the hospitality of the Theory Group of the Lawrence Berkeley Laboratory's Nuclear Science Division.

This work was supported by the Director, Office of Energy Research, Division of Nuclear Physics of the Office of High Energy and Nuclear Physics, of the U.S. Department of Energy under Contract DE-AC03-76SF00098.

Appendix

Let the radius vector $R(\theta)$, locating the effective sharp surface of a deformed nucleus, be written as

$$R(\theta) = \frac{R}{\lambda}\,[1+\alpha_2 P_2(\cos\theta)+\alpha_4 P_4(\cos\theta)] \quad , \tag{A1}$$

where R is the equivalent sharp radius and λ is a scale factor ensuring volume conservation and given (without approximation) by

$$\lambda^3 = 1+\frac{3}{5}\,\alpha_2^2+\frac{6}{35}\,\alpha_2^2\alpha_4+\frac{2}{35}\,\alpha_2^3+\frac{1}{3}\,\alpha_4^2+\frac{60}{693}\,\alpha_2\alpha_4^2+\frac{18}{1001}\,\alpha_4^3 \quad . \tag{A2}$$

We confine ourselves to only two deformation parameters, α_2 and α_4, but from then on we work out the relevant interaction formulae either exactly or to a high precision. By working to only the relevant lowest approximation in α_2 and α_4, the formulae can be considerably simplified at the price of some loss of accuracy. We used numerical values for α_2 and α_4 deduced from the compilation of nuclear deformations in ref. 12, as calculated using the Strutinsky shell-correction method. These values (which exhibit peculiarities associated with the finiteness of the grid used in the configuration space) are only approximate representations of experimental values (where these are known), but the correspondence is amply adequate for our purposes.

a) *The Proximity Interaction*

As stressed in ref. 8 it is important to refer the proximity interaction with respect to the locations of the central radii C (or central radius vectors $C(\theta)$) of the interacting surfaces. According to ref. 8, p. 144, the relation between $C(\theta)$ and $R(\theta)$ is given by

$$C(\theta) = R(\theta) - \frac{1}{2}\,\kappa b^2 \quad , \tag{A3}$$

where b is the Sussman width (diffuseness) of the surface ($\approx$1 fm) and κ is the total curvature of the surface at the point in question, given by

$$\kappa = \frac{1}{R_\theta} + \frac{1}{R_\phi} \quad . \tag{A4}$$

Here R_θ, R_ϕ are the two principal radii of curvature of the surface specified by eq. (A1). (R_θ refers to the curvature in the plane containing the normal to the surface and the symmetry axis and R_ϕ to the curvature in an orthogonal plane through the normal.)

The formulae for R_θ, R_ϕ may be written as follows:

$$R_\theta(\theta) = \frac{R}{\lambda} \frac{u(\theta)^3}{w(\theta)} \tag{A5}$$

$$R_\phi(\theta) = \frac{R}{\lambda} u(\theta) \frac{\beta_1+\beta_2\cos^2\theta+\beta_3\cos^4\theta}{\beta_1+3\beta_2\cos^2\theta+5\beta_3\cos^4\theta} \quad , \tag{A6}$$

with

$$u(\theta) = [\, \beta_1^2+2\beta_2(\beta_1+2\beta_2)\cos^2\theta+(2\beta_1\beta_3+16\beta_2\beta_3-3\beta_2^2)\cos^4\theta \\ +2\beta_3(8\beta_3-7\beta_2)\cos^6\theta-15\beta_3^2\cos^8\theta]^{1/2} \tag{A7}$$

$$w(\theta) = (\beta_1^2-2\beta_1\beta_2)+6(\beta_1\beta_2+\beta_2^2-2\beta_1\beta_3)\cos^2\theta+3(6\beta_1\beta_3+6\beta_2\beta_3-\beta_2^2)\cos^4\theta \\ +10\beta_3(2\beta_3-\beta_2)\cos^6\theta-15\beta_3^2\cos^8\theta \tag{A8}$$

$$\beta_1 = 1 - \frac{1}{2}\alpha_2 + \frac{3}{8}\alpha_4 \tag{A9}$$

$$\beta_2 = \frac{3}{2}\alpha_2 - \frac{15}{4}\alpha_4 \tag{A10}$$

$$\beta_3 = \frac{35}{8}\alpha_4 \tag{A11}$$

For a sphere, the relation between R and C reduces to

$$C = R - \frac{b^2}{R} \quad . \tag{A12}$$

For the radius R of a nucleus with mass number A we use, as before, the semi-empirical formulae from ref. 8:

$$R = 1.28\, A^{1/3}-0.76+0.8\, A^{-1/3} fm \quad , \tag{A13}$$

$$\gamma = 0.9517[1-1.7826((N-Z)/A)^2] MeV/fm^2 \quad . \tag{A14}$$

The proximity attraction between a deformed fragment specified by $R_1(\theta)$ and a spherical fragment with radius R_2, whose center is located at the point (r,θ), is given approximately by

$$V_P \approx 4\pi\bar{R}b\,\gamma\Phi(\varsigma) \tag{A15}$$

where, according to ref. (8), p. 435, $\bar{R}$ turns out to be given by

$$\bar{R} = \left[\frac{C_{\phi 1}(\theta)C_{\theta 1}(\theta)C_2^{\,2}}{(C_{\theta 1}(\theta)+C_2)(C_{\phi 1}(\theta)+C_2)}\right]^{1/2} \quad . \tag{A16}$$

We have used the notation

$$\varsigma = s/b \quad , \tag{A17}$$

where

$$s = r - C_1(\theta) - C_2 \quad . \tag{A18}$$

In the above estimate we have neglected the small difference in magnitude and direction of the distance between the surfaces as measured along the radius vector and as measured along the normal at the point of least separation (see Fig. 3).

The following approximation to $\Phi(\varsigma)$ for $\varsigma > 0$ is given in ref. 9:

$$\Phi(\varsigma) = \begin{cases} -4.41\ e^{-\varsigma/0.7176} & \text{for } \varsigma \geq 1.9475 \\ -1.7817+0.9270\varsigma+0.01696\varsigma^2-0.05148\varsigma^3 & \text{for } 0 \leq \varsigma \leq 1.9475 \end{cases} \quad . \tag{A19}$$

b) *The Coulomb Interaction*

The interaction between a uniform charge Z_1e inside a surface specified by eq. (A1) and a sphere with total charge Z_2e placed outside the surface at the point (r,θ), is accurately approximated by the multipole expansion

$$V_C(r,\theta) = \frac{Z_1Z_2e^2}{r}\,S(r,\theta) \tag{A20}$$

where

$$S\,(r,\theta) \;=\; 1 + \frac{3}{5}\left(\frac{R_1}{r}\right)^2 f_2 P_2(\cos\theta) + \frac{3}{7}\left(\frac{R_1}{r}\right)^4 f_4 P_4(\cos\theta) +$$

$$+ \frac{1}{3}\left(\frac{R_1}{r}\right)^6 f_6 P_6(\cos\theta) \quad , \tag{A21}$$

with the expansion coefficients

$$f_2 = (\alpha_2 + \frac{4}{7}\alpha_2^2 + \frac{6}{7}\alpha_2^3 + \frac{8}{7}\alpha_2\alpha_4 + \frac{72}{77}\alpha_2^2\alpha_4 + \frac{200}{693}\alpha_4^2 + \frac{1028}{429}\alpha_2\alpha_4^2$$

$$+ \frac{400}{1001}\alpha_4^3)\,\frac{1}{\lambda^5} \tag{A22}$$

$$f_4 = (\frac{6}{5}\alpha_2^2 + \frac{12}{11}\alpha_2^3 + \frac{7}{9}\alpha_4 + \frac{40}{33}\alpha_2\alpha_4 + \frac{1789}{429}\alpha_2^2\alpha_4 + \frac{162}{429}\alpha_4^2$$

$$+ \frac{300}{143}\alpha_2\alpha_4^2 + \frac{2645}{2431}\alpha_4^3 + \cdots)\frac{1}{\lambda^7} \tag{A23}$$

$$f_6 \;=\; (\frac{216}{143}\alpha_2^3 + \frac{360}{143}\alpha_2\alpha_4 + \frac{80}{143}\alpha_4^2 + \frac{648}{143}\alpha_2^2\alpha_4 + \frac{11800}{2431}\alpha_2\alpha_4^2$$

$$+ \frac{64480}{46189}\alpha_4^3 + \cdots)\,\frac{1}{\lambda^9} \quad . \tag{A24}$$

c) *Alternative Form of the Shell-Attenuation Function*

The "parabolic" attenuation function $1 - \frac{c^2}{C^2}$ (eq. (11)) tends to zero with a finite slope at $c = C$. an example of a possibly preferable function, which approaches zero smoothly, is

$$\left(1 - \frac{c^2}{C^2}\right)^2 \quad . \tag{A25}$$

Expressing c in terms of V_{int} and then in terms of V_P, as before, we obtain the following "quartic" bell-shaped attenuation function:

$$\left(1 + \frac{2V_P}{E_e}\right)^2$$

$$= \left(1 + \frac{2\overline{R}b\,\Phi(\varsigma)}{C^2}\right)^2 \quad . \tag{A26}$$

When the proximity interaction in small, this function damps out a shell effect twice as fast as the

parabolic one, although eventually they both give total damping at the same value of ς. In the numerical example used in the text (of a ^{208}Pb nucleus in contact with ^{14}C), the Pb shell effect of –13.42 MeV would now be damped by 24% instead of 13%, while the ^{14}C shell effect would be essentially wiped out in both cases. A more general, one-parameter family of attenuation functions, of which the above examples are two special cases, is

$$\left(1 + \frac{2\bar{R}b\,\Phi(\varsigma)}{C^2}\right)^n \quad , \quad \text{for} \quad \left(1 + \frac{2\bar{R}b\,\Phi(\varsigma)}{C^2}\right) > 0$$

$$0 \quad , \quad \text{for} \quad \left(1 + \frac{2\bar{R}b\,\Phi(\varsigma)}{C^2}\right) \leq 0 \quad , \tag{A27}$$

with n an adjustable parameter. It remains to be seen which one of such phenomenological attenuation functions will turn out to be more nearly quantitative.

References

1. D.N. Poenaru, M. Ivascu, A. Sandulescu and W. Greiner, Phys. Rev. C **32**, 572 (1985).
2. D.N. Poenaru, W. Greiner, K. Depta, M. Ivascu, D. Mazilu and A. Sandulescu, Atomic Data and Nuclear Data Tables, in press.
3. S.W. Barwick, "Observation of Novel Radioactive Decay by Spontaneous Emission of Complex Nuclei," Ph.D. Thesis, Department of Physics, University of California at Berkeley, May 14, 1986.
4. Yi-Jin Shi and W.J. Swiatecki, Phys. Rev. Lett. **54**, 300 (1985).
5. Yi-Jin Shi and W.J. Swiatecki, Nucl. Phys. **A438**, 450 (1985).
6. W.D. Myers and W.J. Swiatecki, Nucl. Phys. **81**, 1 (1966).
7. W.D. Myers, "Droplet Model of Atomic Nuclei," IFI/Plenum, New York-Washington-London, 1977.
8. J. Blocki, J. Randrup, W.J. Swiatecki and C.F. Tsang, Ann. of Phys. **105**, 427 (1977).
9. J. Blocki and W.J. Swiatecki, Ann. of Phys. **132**, 53 (1981).
10. W.J. Swiatecki, Progr. Particle Nucl. Phys. **4**, 383 (1980).
11. A. Rytz, Atomic Data and Nuclear Data Tables **12**, 479 (1973).
12. P. Moller and J.R. Nix, Atomic Data and Nuclear Data Tables **26**, No. 2, March 1981.

Figure Captions

Fig. 1. The logarithm of the branching ratio of exotic to α-decay for 15 nuclei arranged in order of increasing mass number. The parent nuclei and emitted isotopes are indicated on the abscissa.

Fig. 2. Comparison of calculated penetrability factors for exotic decay with empirical values deduced by dividing the observed half-life by a pre-exponential factor τ_0 (equal to 10^{-22}sec for even-A emitters and 10^{-20}sec for odd-A emitters). Abscissa as in Fig. 1. Note the false zero on the ordinate.

Fig. 3. Schematic illustration of a deformed parent nucleus decaying to a deformed daughter by α emission, or to a spherical daughter by heavy-ion (exotic) decay. In the former case, what is referred to as "contact configuration" corresponds in fact to a very slight overlap.

Fig. 4. The empirical pre-exponential factor τ_0, obtained by dividing the observed half-life by the calculated penetrability factor G. Deviations of the lines from a constant illustrate the imperfections of the theory. Note the odd-even effect in τ_0, equivalent to a hindrance by about one power of 10 for odd-A α-emitters and about 2 powers of 10 for odd-A exotic radioactivity.

Fig. 5. The effect on the empirical exotic pre-exponential factors τ_0^X of the shell-attenuation effect (upper part) and of parent deformation (lower part). Dashed lines refer to the "old" uncorrected calculations.

Fig. 6. This is like Fig. 1, but with shell-attenuation and deformation corrections included. The inset repeats the plot with a true zero on the ordinate in order to illustrate the relative smallness of the remaining deviations between theory and experiment.

Table I

Properties of 15 exotic radioactivities.

Decay	Experimental branching ratio* τ^{α}/τ^{x}	τ^{α}(sec)†	τ^{x}(sec)	Penetrability integral G_x Old	New	Parent deformation‡ α_2	α_4
$^{221}Fr \rightarrow ^{207}Tl + ^{14}C$	$<5.0\times10^{-14}$	4.8 min	$>5.76\times10^{15}$	1.069×10^{35}	2.054×10^{36}	0.0659	0.0579
$^{221}Ra \rightarrow ^{207}Pb + ^{14}C$	$<1.2\times10^{-13}$	30 sec	$>2.5\times10^{14}$	5.212×10^{33}	1.121×10^{35}	0.0659	0.0579
$^{222}Ra \rightarrow ^{208}Pb + ^{14}C$	$(3.7\pm0.5)\times10^{-10}$	38 s	1.03×10^{11}	1.687×10^{32}	3.817×10^{33}	0.0703	0.0584
$^{223}Ra \rightarrow ^{209}Pb + ^{14}C$	$(6.1\pm1.0)\times10^{-10}$	11.4 d	1.61×10^{15}	6.715×10^{34}	9.146×10^{35}	0.0934	0.0756
$^{224}Ra \rightarrow ^{210}Pb + ^{14}C$	$(4.3\pm1.2)\times10^{-11}$	3.6 d	7.23×10^{15}	6.980×10^{37}	5.971×10^{38}	0.0980	0.0764
$^{225}Ca \rightarrow ^{211}Bi + ^{14}C$	$<4.0\times10^{-13}$	10 d	$>2.16\times10^{18}$	1.519×10^{39}	8.988×10^{39}	0.1027	0.0819
$^{226}Ra \rightarrow ^{212}Pb + ^{14}C$	$(2.5\pm1.0)\times10^{-11}$	1.6×10^{3}y	2.02×10^{21}	4.157×10^{43}	1.506×10^{44}	0.1027	0.0819
$^{230}Th \rightarrow ^{206}Hg + ^{24}Ne$	$(5.6\pm1.0)\times10^{-13}$	7.7×10^{4}y	4.34×10^{24}	2.513×10^{47}	8.024×10^{46}	0.1257	0.0814
$^{231}Pa \rightarrow ^{207}Tl + ^{24}Ne$	6×10^{-12}	3.2×10^{4}y	1.68×10^{23}	9.540×10^{43}	5.466×10^{43}	0.1257	0.0862
$^{232}Th \rightarrow ^{206}Hg + ^{26}Ne$	$<6\times10^{-11}$	1.4×10^{10}y	$>7.36\times10^{27}$	8.234×10^{50}	2.386×10^{50}	0.1303	0.0775
$^{232}U \rightarrow ^{208}Pb + ^{24}Ne$	$(2.0\pm0.5)\times10^{-12}$	72 y	1.14×10^{21}	1.445×10^{42}	1.055×10^{42}	0.1303	0.0872
$^{233}U \rightarrow ^{208}Pb + ^{25}Ne$	$(7.5\pm2.5)\times10^{-13}$	1.6×10^{5}y	6.73×10^{24}	5.345×10^{44}	4.469×10^{44}	0.1303	0.0872
$^{237}Np \rightarrow ^{207}Tl + ^{30}Mg$	$<4\times10^{-14}$	2.1×10^{6}y	1.66×10^{27}	7.262×10^{48}	6.939×10^{47}	0.1349	0.0785
$^{240}Pu \rightarrow ^{206}Hg + ^{34}Si$	$<4.5\times10^{-14}$	6.5×10^{3}y	4.56×10^{24}	5.110×10^{49}	6.196×10^{48}	0.1442	0.0615
$^{241}Au \rightarrow ^{207}Tl + ^{34}Si$	$<3\times10^{-15}$	433 y	4.55×10^{24}	1.036×10^{47}	3.157×10^{46}	0.1442	0.0615

* Ref 3 and private communication from S.W. Barwick

† Ref 11

‡ Ref 12

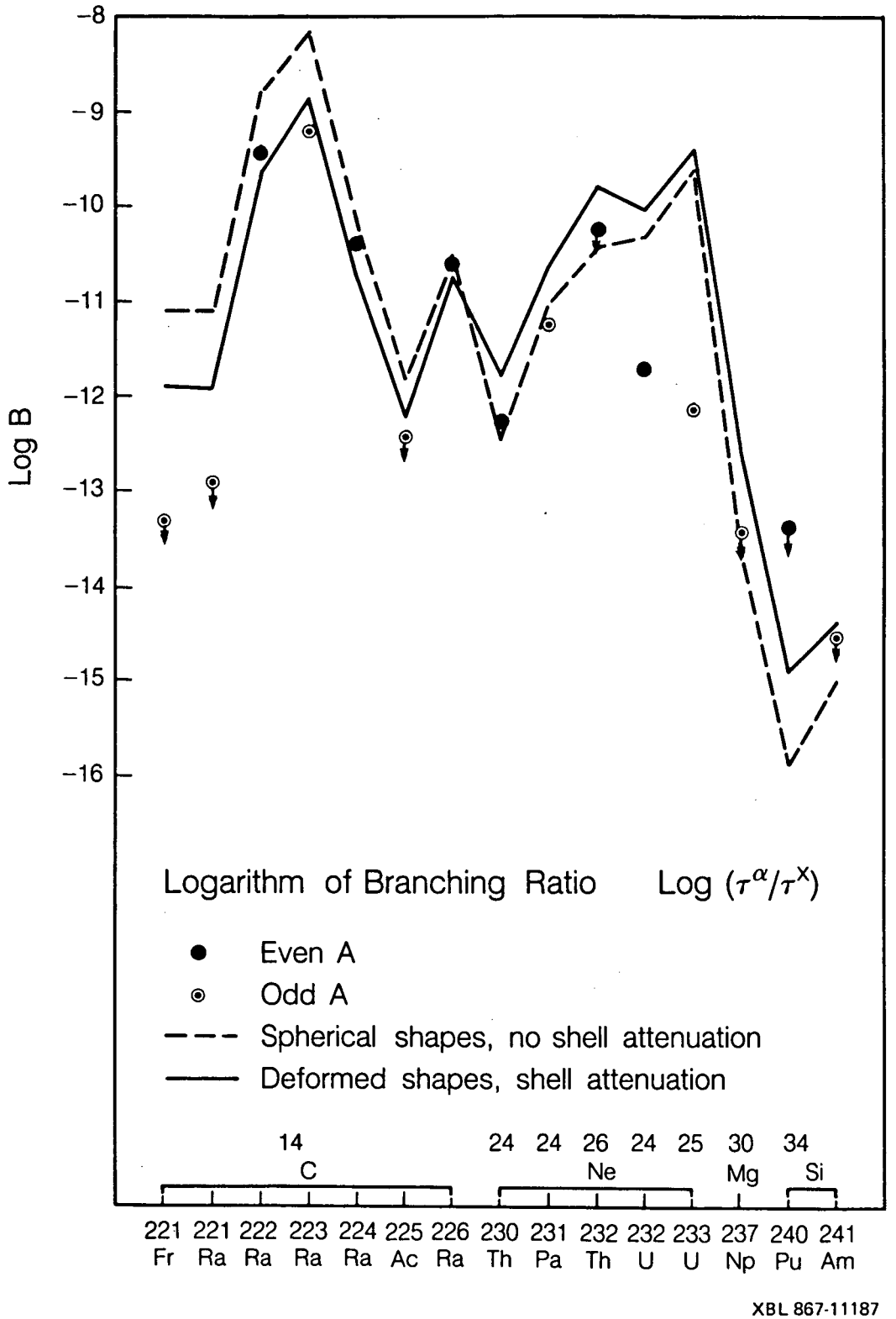

XBL 867-11187

Fig. 1

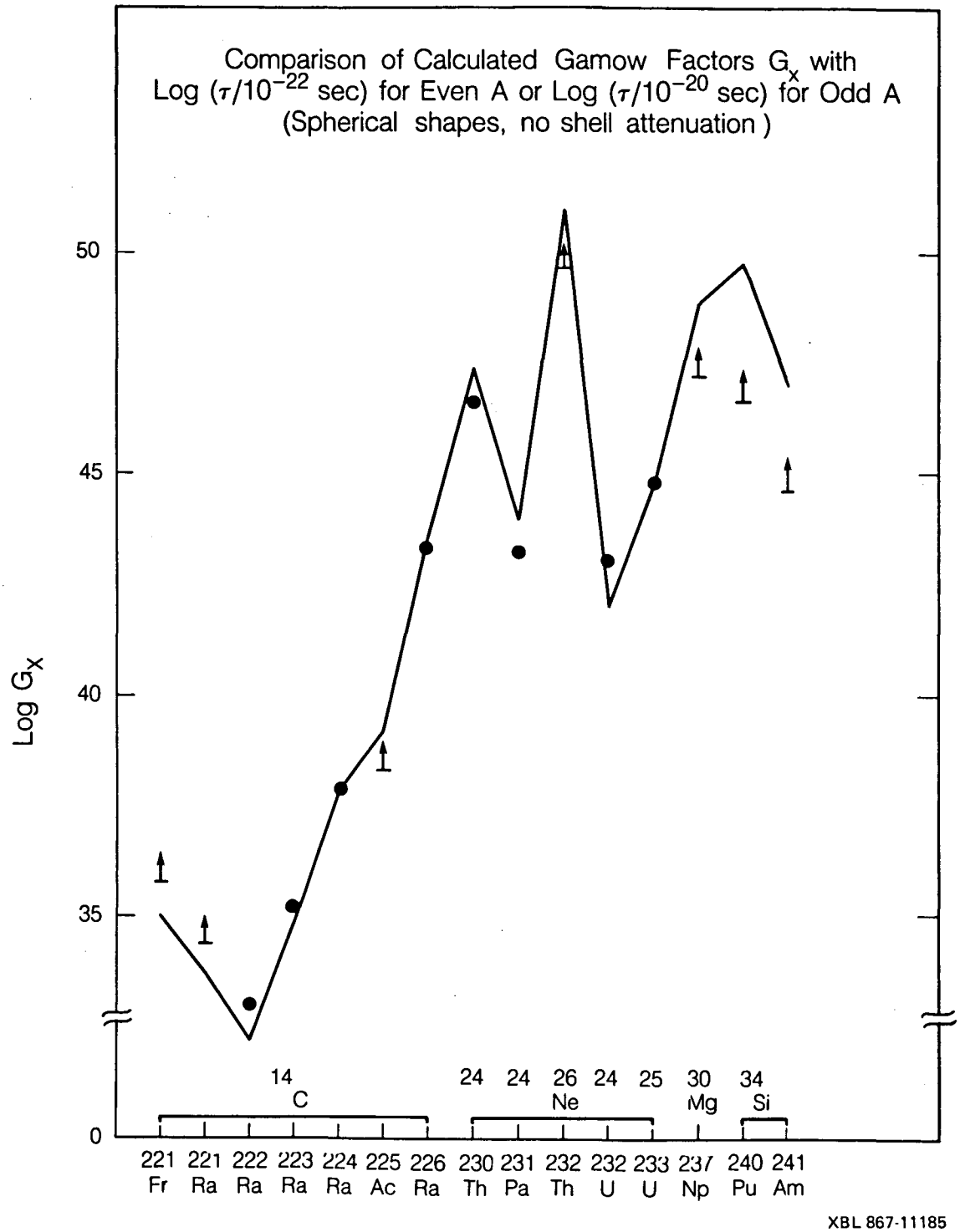
Comparison of Calculated Gamow Factors G_x with
Log ($\tau/10^{-22}$ sec) for Even A or Log ($\tau/10^{-20}$ sec) for Odd A
(Spherical shapes, no shell attenuation)
Log G_X
50
45
40
35
0
14
C
24 24 26 24 25
Ne
30
Mg
34
Si
221 Fr
221 Ra
222 Ra
223 Ra
224 Ra
225 Ac
226 Ra
230 Th
231 Pa
232 Th
232 U
233 U
237 Np
240 Pu
241 Am
XBL 867-11185

Fig. 2

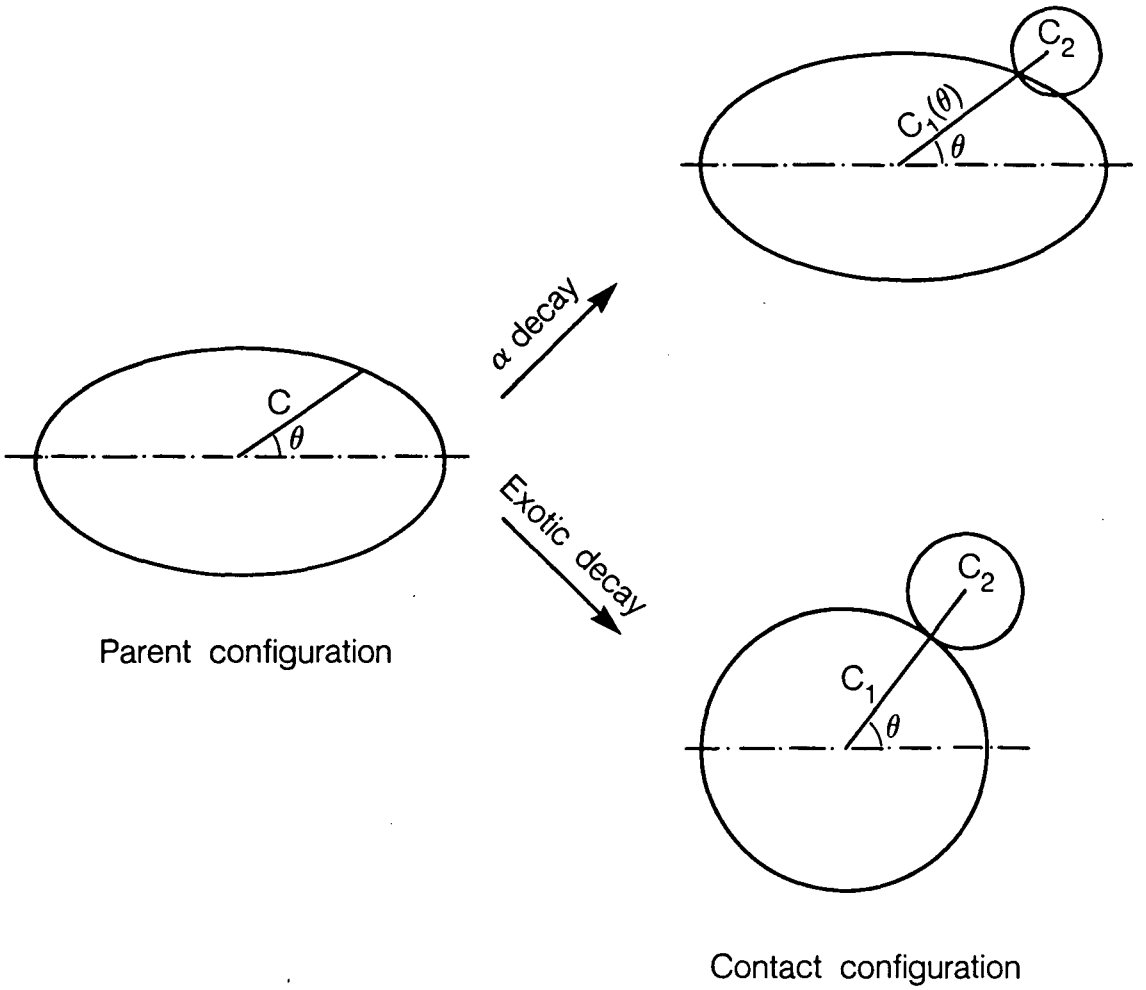

XBL 867-11183

Fig. 3

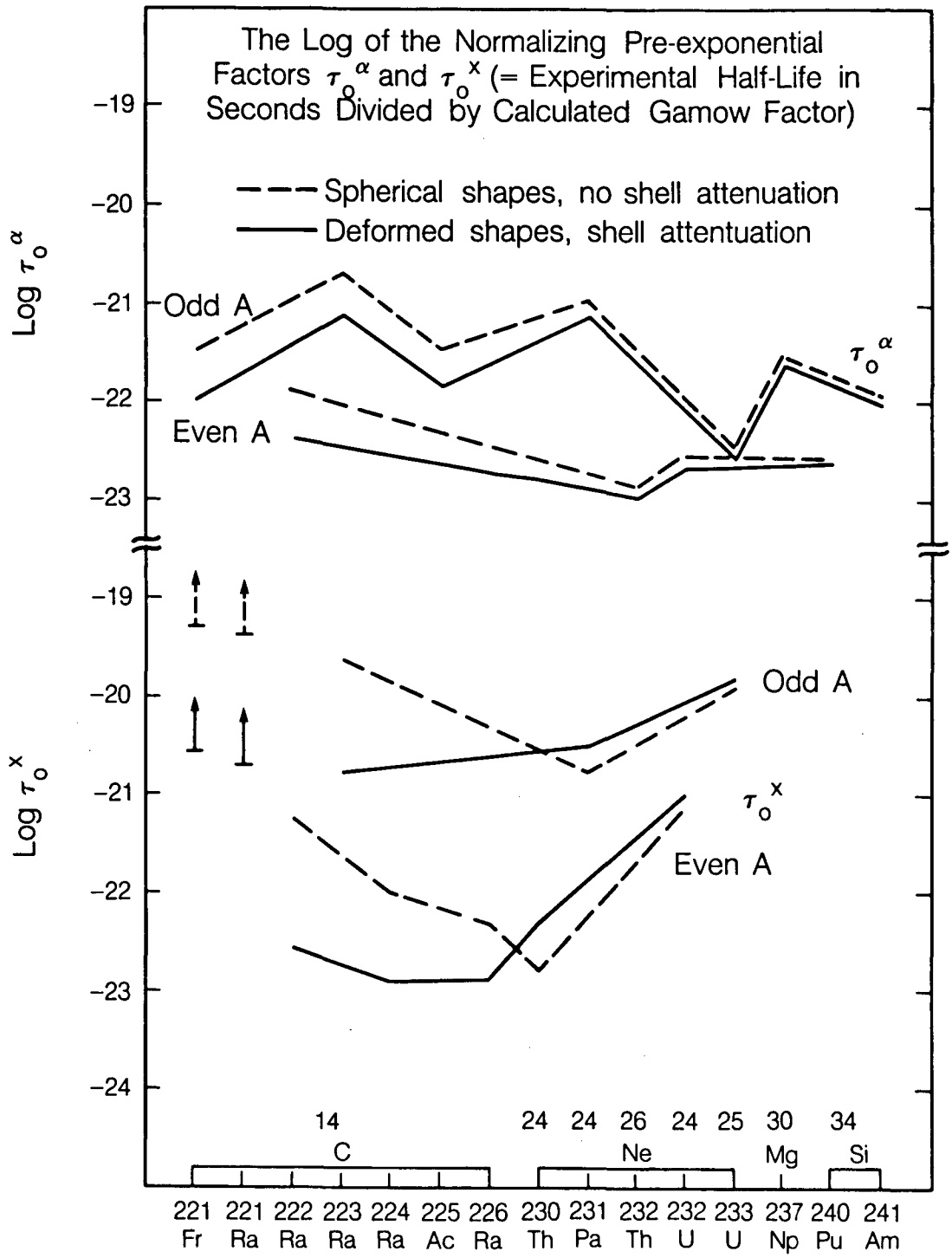

XBL 867-11184

Fig. 4

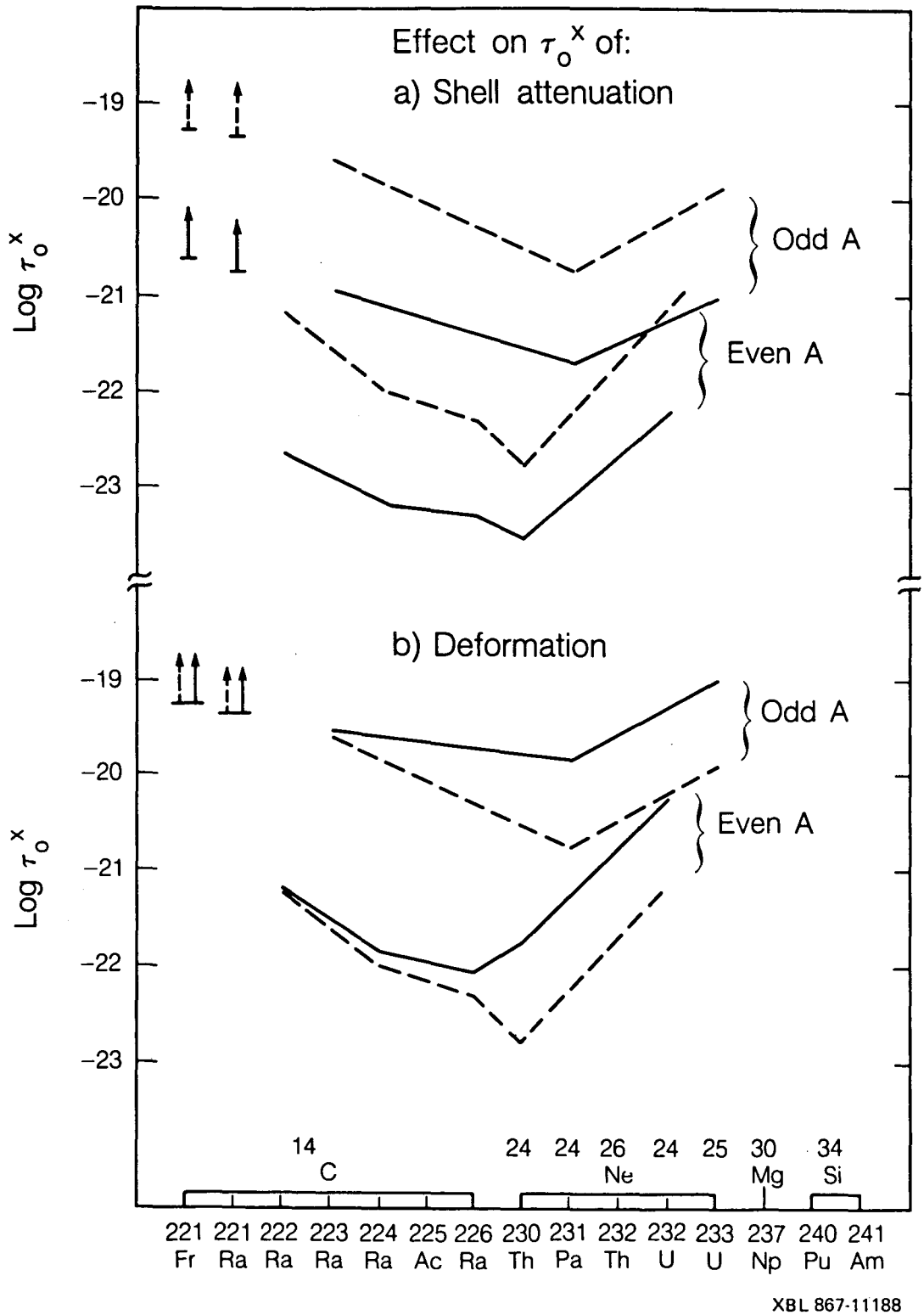
Effect on τ_o^x of:
a) Shell attenuation
b) Deformation
Log τ_o^x
-19
-20
-21
-22
-23
Odd A
Even A
14
C
24 24 26 24 25 30 34
Ne
Mg
Si
221 221 222 223 224 225 226 230 231 232 232 233 237 240 241
Fr Ra Ra Ra Ra Ac Ra Th Pa Th U U Np Pu Am
XBL 867-11188

Fig. 5

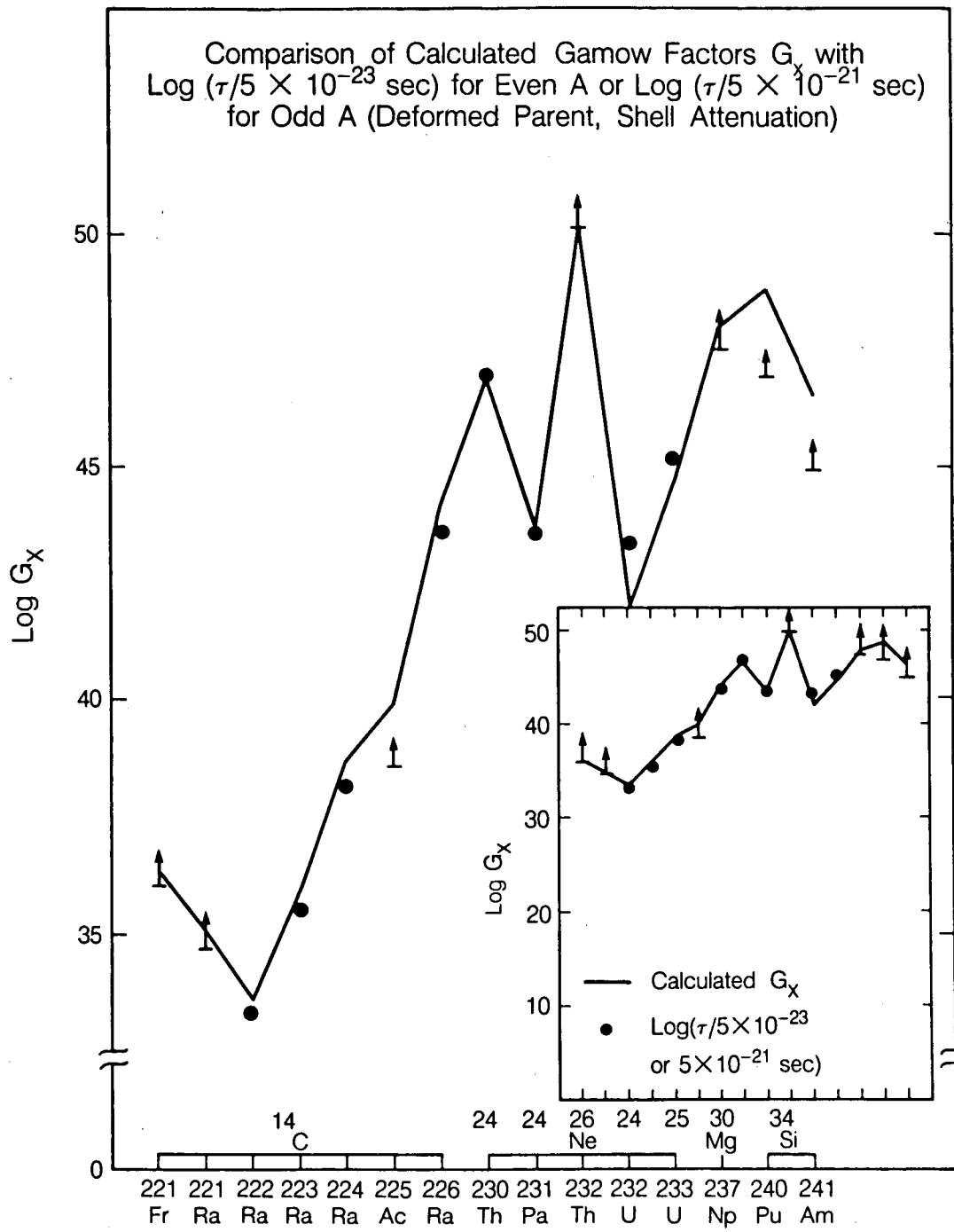

XBL 867-11186

Fig. 6

This report was done with support from the Department of Energy. Any conclusions or opinions expressed in this report represent solely those of the author(s) and not necessarily those of The Regents of the University of California, the Lawrence Berkeley Laboratory or the Department of Energy.

Reference to a company or product name does not imply approval or recommendation of the product by the University of California or the U.S. Department of Energy to the exclusion of others that may be suitable.

LAWRENCE BERKELEY LABORATORY
TECHNICAL INFORMATION DEPARTMENT
UNIVERSITY OF CALIFORNIA
BERKELEY, CALIFORNIA 94720